# X-ray Irradiance Distribution for an Interferometer with a Curved Biprism Array

Grant T. Gullberg,[1,2] Michael Fuller,[3] and Youngho Seo,[2]

[1]Lawrence Berkeley National Laboratory,
Molecular Biophysics and Integrated Bioimaging Division,

[2]UCSF Physics Research Laboratory,
Department of Radiology and Biomedical Imaging,

University of California San Francisco, CA, USA
[3]TF Instruments, Salinas, CA, USA

Technical Report LBNL- 2001601
Lawrence Berkeley National Laboratory
June 24, 2024

## Abstract

The development of interferometry-based X-ray phase contrast imaging systems that provide highly resolved X-rays with spatially-modulated intensity is enabling the full potential of X-ray optics to image phase, attenuation, and small angle scatter properties of soft tissue. In this work we present analytical formulations of a new hardware concept for X-ray phase contrast imaging wherein the phase grating is replaced with an array of Fresnel biprisms. We derive expressions for the irradiance distribution pattern of a biprism interferometer composed of a curved biprism array with multiple biprisms and multiple point sources. These expressions are used to plot fringe patterns for X-ray design parameters, including 1) size, number, and period of X-ray point sources; 2) biprism parameters of material composition, angle, number, and period; and 3) biprism array to X-ray source and detector distances. Analytical results show that the biprism interferometer provides a longitudinally-nonperiodic pattern of spatially modulated intensity different from the Talbot longitudinally-periodic pattern common in grating interferometry. The curvature of the biprism array brings a sharper longitudinal fringe pattern. Experiments are being performed to verify the analytical calculations for a biprism plastic material of SU-8 using a synchrotron source. X-ray biprism material has widely varied indexes of refraction relative to wavelength and thus the separation of the virtual sources and resulting interference fringe period also varies with X-ray wavelength. Our aim is to develop biprism interferometry imaging systems with excellent polychromatic performance that produce high-contrast fringes with spatially incoherent X-ray illumination. Biprism interferometry will potentially provide higher fringe visibility with better image quality to that of diffraction grating interferometry.

Key words: Fresnel biprism, interferometry, Talbot carpet, X-ray phase contrast imaging, dark field imaging

# Preface

This material was presented as a poster at the 2023 IEEE Nuclear Science Symposium and Medical Imaging Conference (NSS/MIC) in Vancouver, B.C, Canada, November 4-11, 2023. The abstract was published by IEEE but none of the other material presented in this lab report has been published.

## I. INTRODUCTION

Interferometry-based X-ray imaging can provide excellent soft-tissue contrast [1] of phase, attenuation, and small angle scatter information of tissue properties. This is feasible even with a conventional X-ray tube by using a Talbot–Lau interferometer with gratings [2], also known as grating based differential phase-contrast imaging (DPCI). Our aim is to develop a new hardware concept for X-ray phase contrast imaging wherein the phase grating is replaced with an array of Fresnel biprisms (Figure 1). It has been demonstrated [3] with a synchrotron source that a Fresnel biprism can produce high-contrast fringes with spatially incoherent X-ray illumination. In a previous study [4] we modified the development for optical wave lengths in [5] to obtain analytical expressions for the irradiance distribution of X-ray sources illuminating a planar array of Fresnel biprisms. In the following section, we develop expressions for the irradiance distribution pattern of X-ray sources illuminating a curved array of biprisms (Figure 1). We use these expressions to plot the distribution of fringes for different parameters of our proposed biprism interferometry system and show that the biprism interferometer provides a longitudinally-nonperiodic pattern of spatially modulated intensity different from the Talbot longitudinally-periodic pattern common in grating interferometry.

## II. ANALYTICAL EXPRESSION FOR THE IRRADIANCE DISTRIBUTION

Assuming an X-ray beam proceeding from a spatially incoherent planar source with wavelength λ illuminates a biprism, we write the irradiance distribution $I$ of X-ray sources on an arbitrary plane placed at a distance z beyond the biprism as [5]

$$I(\vec{x}, Z; \eta) = \frac{\eta^2}{Z^2} I_S\left(\frac{-\eta\vec{x}}{Z}\right) \otimes_2 I_0(\vec{x}, Z; \eta)\ , \tag{1}$$

where $\eta$ is the distance between the source and the bi-prism, $Z$ is the distance between the biprism and the imaging plane, $\otimes_2$ is the 2D convolution performed over the transverse coordinates $\vec{x} = (x, y)$, and $I_S$ is the irradiance distribution of a single X-ray source.

For a spherical wavefront proceeding from a point source illuminating a Fresnel biprism, the exiting wavefront produces an interference pattern $I_0$ beyond the Fresnel biprism whose irradiance distribution is

$$I_0(\vec{x}, Z; \eta) = 1 + cos\left(\frac{2\pi x}{p}\right),$$

where $p = \lambda(\eta + Z)/(2\eta tan\alpha) = \lambda(\eta + Z)/[2\eta tan(\delta tan\chi)]$ is the period of the interference pattern, $\alpha = \delta tan\chi$ is the angle of the beam deflection [5], $\delta$ is the refraction index decrement, and $\chi$ is the angle of the biprism.

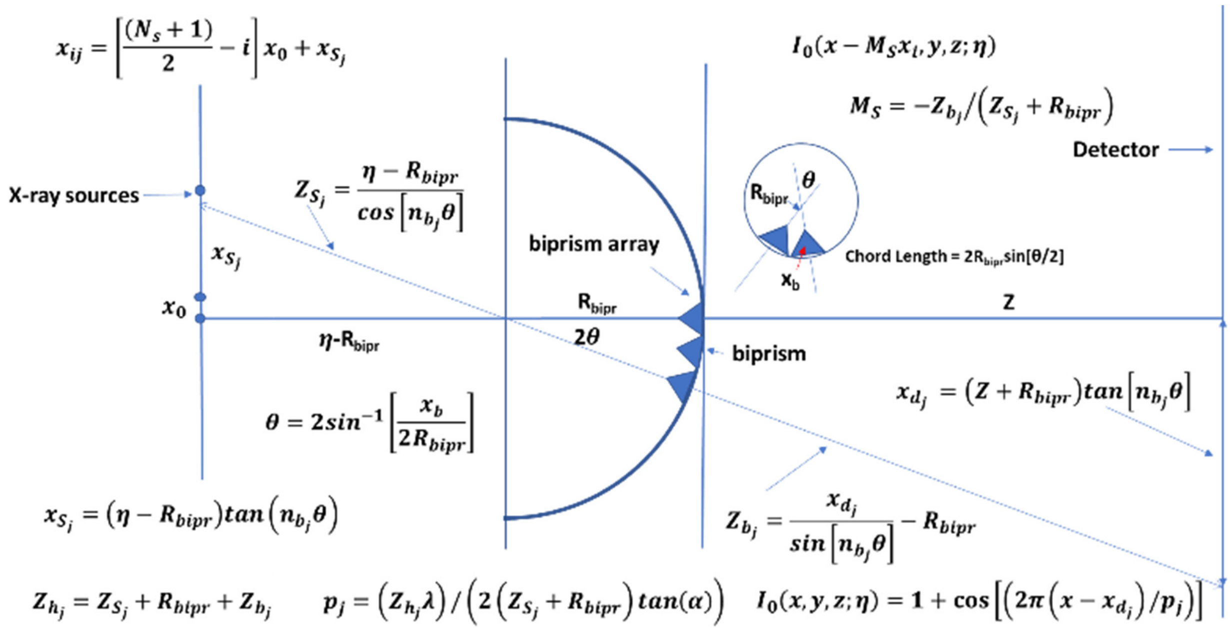


Fig. 1. Geometry of a curved biprism array. The array of biprisms has a radius of $R_{bipr}$. The distance between the central X-ray source and the central biprism is equal to $\eta$ and Z is the distance from this biprism to the detector. (See text for definition of parameters.)

For the case of special interest, the quasi-monochromatic source is composed of an array of $N_s$ mutually incoherent point sources with the same irradiance, $I_P$, and arranged equidistant perpendicular to the plane tangent to circular biprism array and symmetrically to the optical axis. In a realistic experimental situation, the width $\Delta$ of the source along the x- and y-direction would not be infinitesimal. In this case, the irradiance distribution of each source can be written as the convolution between a delta function and a rectangular function of width delta:

$$I_S(x, y) = I_P \delta(x, y) \otimes_2 \prod\left({}^{x}/_{\Delta}, {}^{y}/_{\Delta}\right) ,$$

$$\Pi(x, y) = \begin{cases} 1 & if\ |x| and\ |y| < \frac{1}{2} \\ 0 & otherwise \end{cases} .$$

We assume the sources are located with x-coordinatess $x_i = [(N_s + 1)/2 - i]x_0$ , $i = 1, \ldots\ldots, N_s$ ; where $x_0$ is the separation between neighbor sources. The irradiance distribution of each point source beyond the biprism is :

$$I_{S_i}(x, y, Z; \eta, x_i) = \frac{\eta^2}{Z^2} I_S\left(\frac{-\eta x}{Z} - x_i, \frac{-\eta y}{Z}\right) \otimes_2 I_0(x, y, Z; \eta)$$

$$= \frac{\eta^2}{Z^2} I_S\left(\frac{-\eta x}{Z} - x_i, \frac{-\eta y}{Z}\right) \otimes_2 \left[1 + cos\left(\frac{2\pi x}{p}\right)\right] ,$$

where $-Z/\eta$ is the magnification factor. The irradiance distribution of all the sources is

$$I(x, y, Z; \eta) = \frac{\eta^2}{Z^2} \sum_{i=1}^{N_s} I_{S_i}(x, y, Z; \eta, x_i) \ .$$

This gives an equation for one biprism with multiple point sources. To obtain an expression for multiple biprisms, we sum the irradiance distribution of $N_b$ shifted biprisms separated by $x_b$ obtaining the expression

$$I(x,y,Z;\eta) = \sum_{j=1}^{N_b} \sum_{i=1}^{N_S} I_{S_i}[x - ((N_b+1)/2 - j)x_b, y, Z; \eta, x_i] \ .$$

The previous expression provides the irradiance distribution for a planar array of biprisms illuminated by a plane of X-ray sources. In the following we assume the biprism array is curved as shown in Figure 1. Using the same expression for $I_0$, we need to obtain an expression for $x$ and $p$ using the following expressions:

**1)** The biprism array has a flat side equal to $x_b$, therefore the angle sepation between the centers of the biprism on a curved array is $\theta = sin^{-1}\left[x_b/\left(2R_{bipr}\right)\right]$.

**2)** The distance $x_{s_j}$ where a ray passing through the center of the biprism intersects the plane of sources is located at $x_{s_j} = \left(\eta - R_{bipr}\right) tan\left(n_{b_j}\theta\right)$, where $n_{b_j} = ((N_b+1)/2 - j)$. This is the center $x_{ij}^S = [(N_s+1)/2 - i]x_0 + x_{s_j}$ for the offset of the distributed point sources for the biprism $j$.

**3)** Next, we need the total distance $Z_{h_j} = Z_{s_j} + R_{bipr} + Z_{b_j}$ for a ray passing from the source plane, through center of the circle with radius $R_{bipr}$ of the circular biprism array, through the center of the biprism, and intersecting the detector plane:

$$Z_{s_j} = \frac{\eta - R_{bipr}}{cos\left[n_{b_j}\theta\right]},$$

$$Z_{b_j} = \frac{x_{d_j}}{sin\left(n_{b_j}\theta\right)} - R_{bipr} \ ,$$

$$p_j = \left(Z_{h_j}\lambda\right)/\left(2\left(Z_{s_j} + R_{bipr}\right) tan(\alpha)\right).$$

**4)** Next, we need to find the distance $x_{d_j}$ on the detector plane where this ray intersects the detector: $x_{d_j} = \left(Z + R_{bipr}\right) tan\left(n_{b_j}\theta\right)$, where $Z$ is the distance along the optical axis from the central biprism to the detector.

**5)** Therefore,

$$I_0(x,y,Z;\eta) = 1 + cos\left[2\pi\left(x - x_{d_j}\right)/p_j\right]$$

$$p_j = \lambda\, Z_{h_j}/\left[2\left(Z_{s_j} + R_{bipr}\right) tan\alpha\right] = \lambda\, Z_{h_j}/\left[2\left(Z_{s_j} + R_{bipr}\right) tan(\delta tan\chi)\right]$$

**6)** Next, we need to calculate the magnification $M_{S_j}$:

$$M_{S_j} = \frac{-Z_{b_j}}{Z_{s_j} + R_{bipr}}$$

**7)** Now summing over $N_s$ sources, we have the total irradiance distribution of all the sources:

$$I_{S_t}(x, y, z) = \frac{I_P}{M_{S_j}^2} \sum_{i=1}^{N_s} I_S\left(\frac{x}{M_{S_j}} - x_{ij}^s, \frac{y}{M_{S_j}}\right) \otimes_2 \left[1 + cos\left(\frac{2\pi\left(x - x_{d_j}\right)}{p_j}\right)\right].$$

**8)** Now summing over $N_s$ sources and $N_b$ biprisms, we have the total irradiance distribution:

$$I_{total}(x, y, Z) = I_P \sum_{j=1}^{N_b} \sum_{i=1}^{N_s} \frac{1}{M_{S_j}^2} I_S\left(\frac{x}{M_{S_j}} - x_{ij}^s, \frac{y}{M_{S_j}}\right) \otimes_2 \left[1 + cos\left(\frac{2\pi\left(x - x_{d_j}\right)}{p_j}\right)\right],$$

where $M_{S_j} = -Z_{b_j}/Z_{s_j} + R_{bipr}$ is the magnification factor between the source and the intersection of the plane of the detector.

## III. Results

We used Mathematica (Wolfram Research, Champaign, Illinois) to obtain the irradiance distribution patterns shown in Figues. 2 and 3 using the equation given in the previous section for $I_{total}$, and the following parameter values: $N_s$ = 17 number of x ray sources, $\Delta$ = 0.0000008m size of point source, $x_0$ = 0.000005m separation between point sources, $N_b$ = 101 number of bi prisms, $x_b$ = 0.000010m separation between bi prisms, $R_{bipr}$ = 0.21m radius of the bi prism array, $\chi = 85.32 \times 2\,\pi\,/360$ prism angle in radians, $I_p = 1/\Delta^2$ intensity scaling constant, $\delta$ = 0.00000087 refractive index decrement, $\alpha = \delta\, Tan[\chi]$ the angle of the beam deflection in radians, $\lambda$ = 0.000000000071m source wavelength, $\eta$ = 0.53m distance from source to bi-prism, and Z= 1.03m distance between bi-prism array and detector.

## IV. Discussion

Here we derived expressions for the irradiance distribution pattern of X-ray sources illuminating a curved array of biprisms. Comparing Figures 2 and 3 we see that a curved biprism array sharpens the intensity of the high-contrast fringes and moves them toward the X-ray sources. We observe in Figure 4 a longitudinally-nonperiodic pattern of spatially modulated intensity different from the Talbot longitudinally-periodic pattern common in grating interferometry. When the number biprisms is increased, Figure 2 shows high contrast fringes that increase in intensity at 1.04 m. The parameters in Figure 2 are the same as our biprism array used in our laboratory experiments. Here we have derived expressions for the irradiance distribution pattern of X-ray sources illuminating a curved array of biprisms.

Possible benefits of biprism interferometry over grating interferometry include:

• Greater optic-to-detector distance allows placement of the sample/patient after the biprism array.

• Divergent nature of fringes from biprism array allows detection in a single exposure presenting a Moiré pattern [6].

• Better use of a polychromatic X-ray spectrum by the naturally varied offset (wavelength dependent) of the biprism virtual sources.

• Easier manufacturing, straight-forward alignment, and improved throughput.

• The biprism array interferometer improves the signal-to-noise ratio of the original signal and provides a means to measure phase-shifts of introduced objects.

Experiments using a synchrotron source are ongoing to verify the analytical calculations for a biprism plastic material of SU-8.

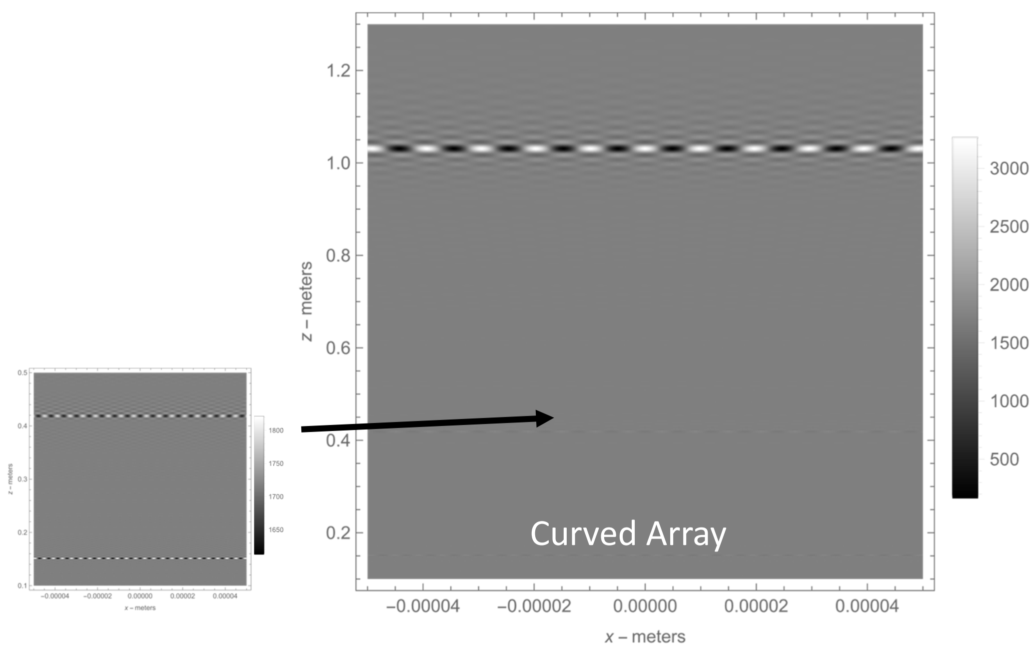


Fig. 2. Irradiance distribution for the curve biprism array shown in Fig. 1. The calculations were performed for 17 X-ray sources ($N_S = 17$) and 101 biprisms ($N_b = 101$).

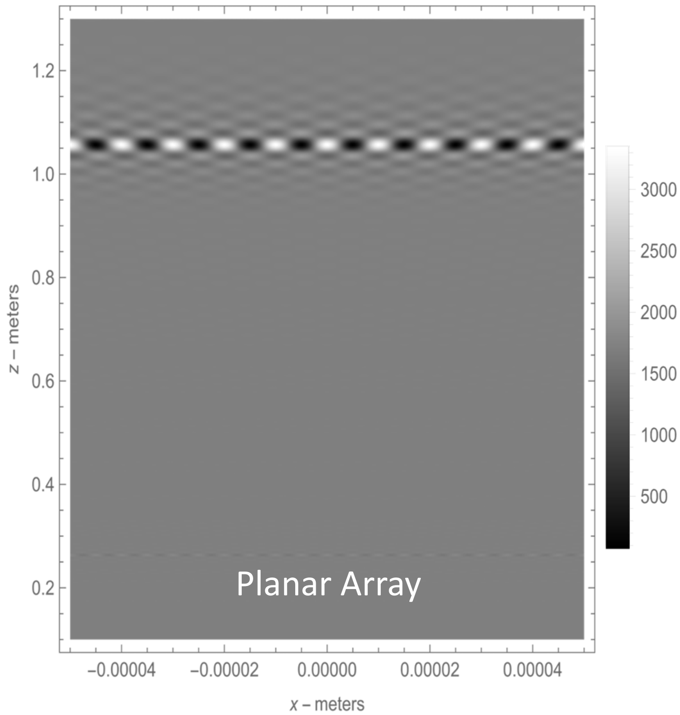


Figure 3. Irradiance distribution for a planar biprism array with same parameters for 1 X-ray souse **($N_S$=17)** and 101 biprisms **($N_b$=101).**

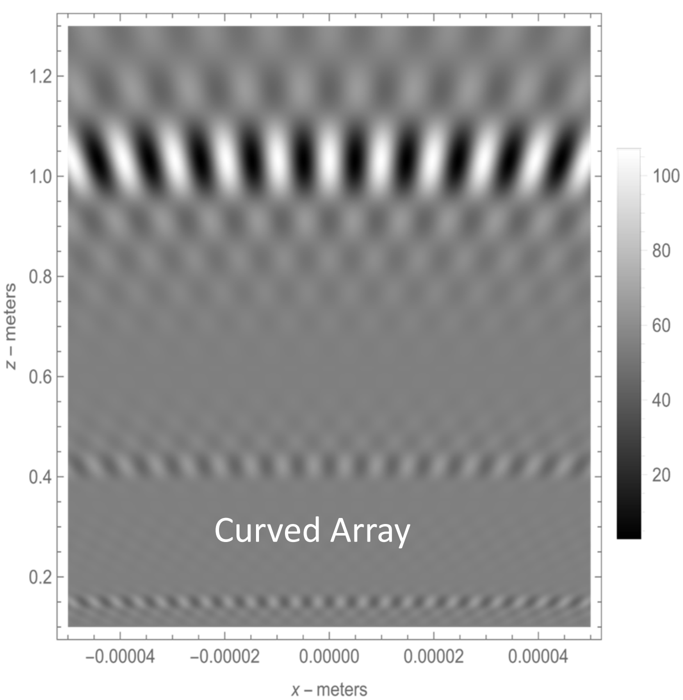


Figure 4. Irradiance distribution for the curve biprism array shown in Figure 1 for 5 X-ray sources **($N_S$=5)** and 11 biprisms **($N_b$=11).**

## References


[1] F. Pfeiffer, O. Bunk, C. David, M. Bech, G. L. Duc, A. Bravin. P. Cloetens, “High resolution brain tumor visualization using three-dimensional x-ray phase contrast tomography,” Phys Med Biol, vol. 52, pp. 6923-30, 2007.

[2] F. Pfeiffer, C. Kottler, O. Bunk, C. David, “Hard x-ray phase tomography with low-brilliance sources,” Phys Rev Lett, vol. 98, pp. 108105-1, -4, 2007.

[3] J. M. Ablett., K. Evans-Lutterodt, A. Stein, “Hard x-rays Fresnel prisms: Properties and applications,” Design and Microfabrication of Novel X-ray Optics II, edited by A. A. Snigirev and D. C. Mancini, Proceedings of SPIE, vol. 5539, August 2, 2004.

[4] G. T. Gullberg, U. Shrestha, S. J. W. Kim, Y. Seo, M. Fuller, “X-ray bi-prism interferometry--A design study of proposed novel hardware,” Med Phys, vol. 48, pp. 6508-6523, 2021.

[5] A. Doblas, G. Saavedra, M. Martinez-Corral, J. C. Barreiro, E. Sanchez-Ortiga. A. Llavador, “Axial resonance of periodic patterns by using a Fresnel biprism,” J Opt Soc Am A, vol. 30, 140-8, 2013.

[6] W. Tao, Y. Sung, S. J. W. Kim, Q. Huang, G. T. Gullberg, Y. Seo, M. Fuller, „Tomography of dark field scatter including single-exposure Moiré fringe analysis with X-ray bi-prism interferometry – A simulation study,” Med Phys, vol. 48, pp. 6293–6311, 2021.